Analysis of Saharan dust intrusions into the Carpathian Basin (Central Europe) over the period of 1979–2011

György Varga[a*], János Kovács[b,c] & Gábor Újvári[d]

[a]Geographical Institute, Research Centre for Astronomy and Earth Sciences, Hungarian Academy of Sciences, Budaörsi út 45, H-1112 Budapest, Hungary (E-mail: varga.gyorgy@csfk.mta.hu)

[b]Department of Geology, University of Pécs, Ifjúság u. 6, H-7624 Pécs, Hungary (E-mail: jones@gamma.ttk.pte.hu)

[c]Environmental Analytical & Geoanalytical Laboratory, Szentágothai Research Centre, University of Pécs, Ifjúság u. 34, H-7624 Pécs, , Hungary

[d]Geodetic and Geophysical Institute, Research Centre for Astronomy and Earth Sciences, Hungarian Academy of Sciences, Csatkai E. u. 6-8, H-9400 Sopron, Hungary (E-mail: ujvari@ggki.hu)

[*]Corresponding author – E-mail: varga.gyorgy@csfk.mta.hu

Abstract

Aeolian dust particles and dust storms play substantial role in climatic and other environmental processes of the Earth system. The largest and most important dust source areas are situated in the Sahara, from where several hundred thousand tons of mineral dust is emitted each year and transported towards the European continent. Here we show that 130 Saharan dust events (SDEs) reached the atmosphere of the Carpathian Basin from 1979 to

2011 by using the NASA’s daily TOMS Aerosol Index data, satellite images and backward trajectory calculations of NOAA HYSPLIT model. Monthly trends of dust events demonstrate that the main period of dust transportation is in the spring, with a secondary maximum in the summer (in July and August). This seasonal distribution match well the seasonality of Saharan dust emissions. However synoptic meteorological conditions govern primarily the occurrence of long-range dust transport towards Central Europe. Based on their different meteorological backgrounds (geopotential field, wind vector and meridional flow), SDEs were classified into three main types. By using composite mean maps of synoptic situations and backward trajectories, the possible source areas have also been identified for the different types of events. Finally, we provide a short discussion on how the African mineral dust could contribute to the local aeolian sedimentation of the Carpathian Basin during the Plio-Pleistocene.

Highlights:

130 Saharan dust events (SDEs) were identified in the Carpathian Basin (CB) atmosphere from 1979 to 2011

Spring and summer are the typical seasons of SDEs

SDEs can be classified in three main types based on synoptic meteorological conditions

Saharan dust could have played a role in loess and red clay sedimentation of the CB during the Plio-Pleistocene

Key words: mineral dust; dust storm; meteorology; Sahara; Carpathian Basin;

1. Introduction

Dust storms and related atmospheric mineral particles have been in the focus of environmental and climatic studies for the last two decades (Stout et al., 2009). Previous investigations confirmed that windblown dust is an active component of the climate system, and can modify its elements via both direct and indirect effects (Harrison et al., 2001; Kohfeld and Tegen, 2007; Maher, 2010; Pósfai and Buseck, 2010). Dust particles affect the Earth's energy balance directly through absorption, scattering and reflection of incoming shortwave and outgoing longwave radiation or by changing the albedo of (bright) surfaces (e.g. Arimoto, 2001). Indirectly, by acting as cloud condensation nuclei, mineral particles have also an effect on atmospheric moisture balance (Rosenfeld et al., 2001; Sassen et al., 2003). Particles rich in Fe have major impact on iron-limited oceanic ecosystems, and thus, dust can influence the primary phytoplankton production and the carbon cycle through biogeochemical interactions (Ridgewell, 2002).

The global annual input of mineral dust deflated from arid-semiarid areas can be set in the range between 1 and 3 billion of tons (Tegen et al., 1996; Mahowald et al., 1999, 2006; Ginoux et al., 2001). Most important sources are situated in Saharan and Sahel regions, which are responsible for 50–70% of the global emission (Ginoux et al., 2001; Miller et al., 2004). Four main pathways of Saharan dust transport can be distinguished: (1) southward to Gulf of Guinea; (2) westward over the North Atlantic Ocean; (3) eastward to Middle East; and (4) northward to Europe (for more details, see Engelstaedter et al., 2006; Goudie and Middleton, 2006).

The several hundred thousand tons of dust derived from Saharan sources influence numerous constituents of European environmental systems (D'Almeida, 1986; Prospero, 1996). During heavy dust-outbreaks, atmospheric dust concentration often exceed PM_{10} standards of the European Union in Spain (Rodríguez et al., 2001), in Italy (Matassoni et al., 2011) and in

Greece (Gerasopoulus et al., 2006), thereby affecting human health (Griffin et al., 2001). The strongly alkaline dust particles increase the pH of precipitation, thus reduce the frequency of acid rains (Roda et al., 1993; Rogora et al., 2004; Špoler Čanić et al., 2009). As proposed by Psenner (1999), permanent Saharan dust contributions to low-alkalinity European lakes prevented them to become acidic during the late twentieth century. The accumulated dust particles are even capable of modifying soil properties of a given region (Yaloon, 1997). As such, terra rossa soils in Portugal (Jahn et al., 1991), in Spain (Muhs et al., 2010), in Italy (Jackson et al., 1982), in Croatia (Durn et al., 1999), in Greece (MacLeod, 1980) and in Turkey (Atalay, 1997) have been shown to be an alteration product of local material and far-travelled African mineral dust.

Fine-grained particles lift to higher levels of the atmosphere and have a long atmospheric residence time up to a few weeks (Pye, 1987). Aeolian dust from North Africa can often be detected in Europe's high-latitude areas e.g. in British Isles (Wheeler, 1986), in Germany (Klein et al., 2010), in Scandinavia (Franzén, 1994; Barkan and Alpert, 2010) and even in our study area, the Carpathian Basin (CB) (Central Europe) (Borbély-Kiss et al., 2004; Koltay et al., 2006; Szoboszlai et al., 2009). Nowadays the CB is generally not regarded as a dusty place, except for episodic dust storms related to cold fronts invading the region at the beginning of the vegetation period in the early spring. Still, Central Europe is lying in the D1b zone of the "Saharan dust-fall map" of Stuut et al. (2009), implying that recent Saharan dust material can be incorporated into the soil system and may increase its fine silt content (Stuut et al., 2009). However, dust activity of the region was much more significant during the Plio–Pleistocene periods, as it is shown by thick aeolian dust deposits covering more than half of the area (e.g. Pécsi and Schweitzer, 1993; Kovács et al., 2008, 2011; Újvári et al., 2010; Varga, 2011). It has been recognized that mineral dust particles of these aeolian sediments originate mainly from local sources (e.g. alluvial plains), and only the clay and fine-silt fractions may be linked to Saharan sources (Rózycki, 1991; Rousseau et al., 2007; Újvári et al., 2012), similarly to Italian loess deposits (Cremaschi, 1990a, 1990b).

The present paper is aimed at providing information on the frequency and seasonality of recent Saharan dust intrusions that can reach the CB atmosphere. Besides, our goal is to define the mean synoptic situations, typical transport pathways and source areas of this airborne mineral dust material.

2. Methods

2.1 Establishment of spatial and temporal changes of atmospheric dust using the TOMS Aerosol Index

Satellites represent the only data source with truly global coverage on most important dust source areas and their emissions. For this study the Total Ozone Mapping Spectrometer's (TOMS) aerosol data were employed to estimate atmospheric dust amount. The TOMS aerosol index, as defined by the NASA/GSFC Ozone Processing Team, is a measure of how much the wavelength dependence of backscattered UV radiation from an atmosphere containing aerosols (Mie scattering, Rayleigh scattering, and absorption) differs from that of a pure molecular atmosphere (pure Rayleigh scattering). Quantitatively, the aerosol index AI is defined as

$$AI = 100 \log_{10}\left(\frac{I_{360}^{meas}}{I_{360}^{calc}}\right), \quad (1)$$

where I_{360}^{meas} is the measured 360 nm TOMS radiance, and I_{360}^{calc} is the calculated 360 nm TOMS radiance for a Rayleigh atmosphere (Herman et al., 1997). The TOMS sensors (on board of different sun-synchronous NASA satellites) have the longest available global record (since

1978 November) with appropriate spatial (1×1.25 degree) and temporal (daily) resolution (Herman et al., 1997; Torres et al., 1998).

Analyses of daily data-matrices were performed in MathWorks' MATLAB (R2007b) environment, while kriging of maps was processed in Golden Software SURFER 8 (Fig.1). The fractional data of 1993 and 1996 (caused by satellite failure), the periods with calibration problems of 2001–2004 (Kiss et al., 2007) and 2010–2011, and the four-yearly leap days (due to the matrix-operations) were excluded from the long-term mean mapping analyses (Table 1). Some few dates have not been either available within other periods, so these were replaced by mean values of previous days.

Figure 1.

Table 1.

Data used	**Satellite**	**Time-series**	
01/01/1979–06/05/1993	Nimbus-7	14×365 + 126	5236 days
06/05/1993–25/07/1996	No data		
25/07/1996–31/12/2000	EarthProbe	4×365 + 160	1620 days
01/01/2001–31/12/2004	Calibration problems		
01/01/2005–31/12/2009	Aura/OMI	5×365	1825 days
01/01/2010–31/12/2011	Calibration problems		
01/01/1979–31/12/2011		**23×365 + 286**	**8681 days**

2.2 Identification of Saharan dust events (SDE) over the Carpathian Basin

The daily TOMS AI values of the investigation area (45°–48.5°N, 16°–23°E) were standardized following the work of Barkan et al. (2005):

$$AI_{st} = \frac{(AI - AI_{mean})}{\sigma_{AI}}, \quad (2)$$

where AI_{st} is the daily standardized TOMS AI value, AI_{mean} is the yearly regional mean TOMS AI and σ_{AI} is the standard deviation. Negative AI_{st} indicates below average values, whereas positive values represent possible dusty episodes. During the SDE identification work fractional data of 1993 and 1996, which have been excluded from mean mapping analyses, were also employed. The periods of 2001–2004 and 2010–2011 could not be analysed in the same way, due to calibration problems; for these intervals, the possible SDEs were identified directly from daily TOMS AI maps.

A given supposed SDE is only accepted after being confirmed by satellite images of NOAA AVHRR (Advanced Very High Resolution Radiometer – source: http://www.sat.dundee.ac.uk), ESA Meteosat SEVIRI (Spinning Enhanced Visible and Infrared Imager – source: http://www.sat.dundee.ac.uk) and Terra or Aqua MODIS (Moderate Resolution Imaging Spectroradiometer – source: http://modis.gsfc.nasa.gov), and by backward trajectory calculations of NOAA HYSPLIT (HYbrid Single-Particle Lagrangian Integrated Trajectory) model (Draxler and Rolph, 2012; Rolph, 2012). The meteorological input for the trajectory model was the NCEP/NCAR (National Centers for Environmental Protection/National Center for Atmospheric Research) Reanalysis Project dataset (Kalnay et al., 1996).

2.3 Mean synoptic patterns and typical pathways of SDEs

Daily geopotential height (at 700mb), wind vector and meridional flow data of the identified SDEs were obtained from the NCEP/NCAR Reanalysis project (Kalnay et al., 1996). The selection of 700mb level was based on previous analyses of long-range Saharan dust transport episodes (Hamonou et al., 1999; Barkan et al., 2005; Dayan et al., 2007). These meteorological data were classified according to their synoptic patterns, and composite mean maps of each type were compiled using the Daily Mean Composite application of NOAA Earth System Research Laboratory (http://www.esrl.noaa.gov/psd/). In order to identify the typical dust transportation routes, the daily backward trajectories of all type SDEs were plotted on multiple trajectory maps, using the NOAA HYSPLIT model (Draxler and Hess, 1997).

3. Results and discussion

3.1 Frequency of Saharan dust intrusions into the Carpathian Basin

During the investigation period of 1979–2011 130 Saharan dust episodes could be identified in the CB atmosphere. The time series of annual number of SDEs are characterized by high amplitude annual variations (Fig. 2). Outstanding values of 1984, 1985, 1992, 2000, 2001 and 2008 with 8 or more SDEs are in contrast with the years of 1981, 1991, 2003, 2004, 2006 and 2009, when the number of identified events was far below the average. The causal relationships among the changing annual frequency of SDEs, Saharan and Sahel droughts, climate teleconnections and atmospheric circulation patterns are not yet fully understood. In some cases, the increased number of identified SDEs over the CB is coincident with Saharan drought periods (e.g. in 1983–84), but in other cases this relationship become increasingly uncertain (e.g. in 2008 and 2009).

Figure 2.

Monthly values of dust events demonstrate that the main period of dust transportation is in the spring, with a secondary maximum in the summer (in July and August), and dust activities in February and October are also fairly high (Fig. 3). This seasonality pattern of our observations fairly agrees with reports of several previous studies on Saharan dust events (Moulin et al., 1998; Middleton and Goudie, 2001; Barkan et al., 2005; Engelstaedter et al., 2006; Goudie and Middleton, 2006 and references therein).

It is worth mentioning that, according to the proton-induced X-ray emission analyses and backward air trajectories of Borbély-Kiss et al. (2004) and Koltay et al. (2006), the maxima of SDEs in Hungary appear in March and November. However, some of the identified events of these studies could be originated from the southernmost part of the Sahel or even from the Sudanian savannas, where biomass burning is the most important source of aerosols (Koltay et al., 2006).

Figure 3.

3.2 Synoptic patterns of Saharan dust transport towards the Carpathian Basin

In spring and summer, the thermal convective activity forces the injection of particles to higher atmospheric levels. It was recognized by Israelevich et al. (2002) that during these periods a permanent reservoir of dust exists in the atmosphere above the major source areas, and the occurrence of long-range dust transport is primarily governed by meteorological conditions. Our monthly mean TOMS AI maps also confirmed these findings for the period of 1979–2009 (Fig. 4).

Figure. 4.

However, the strong upper level flows and resulting dust outbreaks can be connected to various meteorological conditions. Based on the daily geopotential height and wind maps, and backward trajectories of the SDEs, three main types of synoptic patterns and dust transport pathways are distinguishable.

3.2.1 Type-1

66.2% (n=86) of the total SDEs belong to Type-1, which is a similar synoptic situation to that mentioned by Barkan et al. (2005) concerning Saharan dust transport towards Italy. In this case, a deep, well-developed trough emanated from the Bay of Biscay to the Atlantic coast of Africa, and the eastern cell of the divided subtropical high over North Africa causes the strong southwestern flow. The composite mean 700mb geopotential height and wind flow maps of the identified Type-1 SDEs represent this situation in detail (Fig. 5). The dust particles penetrate from North Africa into the atmosphere of the CB by strong SW flow across the western or central basin of the Mediterranean Sea.

Seasonality of the identified 86 Type-1 SDEs display similar bimodal pattern compared to the total SDEs. Monthly frequencies of the discussed type are typically high from March through August. This seasonal distribution is the consequence of the synoptic background, as it is the period of the northward migration of the subtropical high-pressure belt (actually a series of high-pressure centres). In June, due to intense heating of the mainland, a low-pressure region develops in Central Europe. The thermal low creates a steady pressure gradient between the land and the Atlantic Ocean (this month is the wettest in the CB), and the resulting persistent NW-flow blocks the penetration of dusty Saharan air masses.

Figure 5.

3.2.2 Type-2

33 SDEs were identified as Type-2 events, which is 25.4% of the total observations. Dust events related to Type-2 are generated by southerly winds associated with depressions centred in the central Mediterranean. The dust transport is generated by warm sector winds on foreside of the eastward moving cyclones (Fig. 6) and the strongest meridional wind flows are located above the Ionian Sea and the southern part of the Apennine Peninsula, suggesting straight dust intrusions from the south into the CB. Mediterranean low-pressure centres are developing and the Type-2 SDEs occur typically in spring, before the intensification of the Azores High caused by northward migration of subtropical highs.

Figure 6.

3.2.3 Type-3

11 episodes (8.5% of the total) were classified as Type-3 SDE, at times when a high pressure centre is established over NW Africa and SW Europe. The strong flows of the anticyclone carry dust particles from western parts of the Sahara northward along the coastline or over the eastern Atlantic, at the mid-latitudes the dust-laden air mass moves eastward due to the westerlies (Fig. 7). This type of Saharan dust transport is responsible for the observed dusty events in western Europe (Pye, 1987): in Ireland (e.g. Tullet, 1978; Vernon and Reville, 1983) and in Britain (e.g. Mill and Lempfert, 1904).

Figure 7.

3.3 Typical pathways of dust transport and possible North African sources of mineral dust

Related to the main synoptic situations, three typical routes of Saharan dust transport can be identified based on the calculated backward trajectories of SDEs (Fig. 8). Type-1 synoptic pattern favours to northeastward dust transport from the NW Sahara across the western basin of the Mediterranean Sea. During Type-2 events, the outbreaks of dust-laden air reach the CB directly from the south, and rarely from the SE. The longest (ca. 6500 km) and least common dust pathways are associated with the Type-3 SDEs from the western parts of Sahara across the eastern Atlantic and western Europe.

Figure 8.

It is clearly visible on the mean aerosol maps that large proportion of emitted Saharan dust can be associated with some distinct source areas situated in topographic lows or on the flanks of topographic highs (Fig. 9; Middleton and Goudie, 2001; Prospero et al., 2002; Washington et al., 2003; Engelstadter et al., 2006). Most of these sources were flooded during the Pleistocene and Holocene pluvial periods, and nowadays can be characterized with ephemeral rivers and streams, alluvial fans, playas and saline lakes favouring the accumulation of fine-grained material. Large sand seas cannot be regarded as effective source areas due to the shorter atmospheric residence time and shorter transport of sand particles. However, the bombardment energy of sand grains can disrupt the hardened and compacted smooth surfaces of salt lakebeds and playas, thereby enhancing the amount of emitted dust particles (Gillette, 1999). Many of these source areas are located in proximity to large sand seas (Prospero et al., 2002).

Figure 9.

The mean aerosol and detailed topographic maps, as well as previous studies (e.g. Prospero et al., 2002) and backward trajectory analyses allows for locating the most probable dust loading regions over North Africa. Extensive areas with high dust activity can be found in the western region of the Sahara. One of these major sources is the territory of a series of playas and seasonal streams (marked with 1 at Fig. 9) at the slopes of Zemmour Massif and Adrar Soutouf Highlands, running parallel to the Atlantic coast. These areas, together with the dust hotspot (2) next to the Inner Niger Delta (Mali) could be the source of mineral dust of Type-1 and seldom Type-3 dusty events of the CB. As this region is often fully obscured by the atmospheric dust, a closer identification of exact locations of different types is difficult.

The large alluvial fans and wadis at the western slopes of Ahaggar Moutains (3) can be characterized by high mean aerosol index and by several trajectories of both Type-1 and Type-2. Furthermore, the depression of Tidikelt at the northern part of this region, surrounded by plateaus (the Tanezrouft to the south and Plateau du Tademait to the north), by mountains (Ahaggar and Tassili-n-Ajjer to the east) and by the sand sea of Erg Chech to the west has an extensive ephemeral drainage system including several wadis from elevated regions, seasonal marshes and mud flats (Glaccum and Prospero, 1980).

Similarly to Tidikelt, the system of salt and dry lakes in the lowlands south of the Tell Atlas (4) acts also as a major source of dust material of both the identified Type-1 and Type-2 SDEs. Dust activity seems to be the largest between and to the south of the two largest salt lakes (Chott Melrhir and Chott Jerid), in the foreland of Grand Erg Oriental (Prospero, J.M. et al., 2002).

The dusty area expanding from the northern hillslopes of Tibesti across Cyrenaica to the Qattara Depression (5) is the easternmost region responsible for SDEs over the CB. These sources are associated with alluvial fans and extensive wadi systems on flanks of topographic highs, and ephemeral salt lakes in the low-lying areas. Dust entrainment from this region towards Central Europe only occurs during the existence of Type-2 synoptic patterns.

It is notable that backward trajectories have not indicated any events originating from the Bodele depression for the entire studied period of 1979–2011, despite the fact that it is considered as the most intense dust source globally (McTainsh and Walker, 1982; Prospero, 2002; Engelstaedter et al., 2006).

3.4 Sahara as a source of Plio-Pleistocene aeolian dust deposits (red clay and loess) in the Carpathian Basin?

As it has been mentioned earlier, in some periods of Earth's history the amount of atmospheric dust and frequency of dust storms increased by several orders of magnitude, compared to the present situation (Mahowald et al., 1999, 2006; Kohfeld and Harrison, 2001). The Pleistocene glacials were such dusty periods that widely distributed, thick loess deposits were formed all over the mid-latitudes (Muhs and Bettis, 2003). Wind-blown loess and loess-like deposits (underlain by aeolian red clay) are covering almost half of the CB (Pécsi 1990). Previous studies (Kovács, 2008; Kovács et al., 2008, 2011; Varga, 2011; Varga et al., IN PRESS) revealed that the bimodal grain-size distribution curves of the aeolian dust deposits of the CB are representing two main sediment populations and may be interpreted as a mixture of local and far-travelled dust material. Recent observations of dust emissions (Pye, 1987,

1995) demonstrated that the coarse-grained (~10–60 μm) component of aeolian dust deposits was transported by surface winds in short suspension episodes, during discontinuous local dust storms. The fine-grained (~1–8 μm) component is generally transported by upper level flows even from remote deflation areas (Pye, 1987; Tsoar and Pye, 1987; Sun et al., 2002, 2004; Stuut et al., 2009).

The more seasonal distribution of precipitation, stronger winds and intensifying cyclogenesis triggered by more frequent incursions of cold Arctic air masses, and the long-term variations of African summer monsoon (Larrasoaña et al., 2003) led to increased dust emissions from the Sahara during glacial phases. Analyses of Mediterranean marine sediments also confirmed the enhanced wind-blown dust supply from the Sahara during cold periods (Moreno et al., 2002; Hoogakker et al., 2004; Larrasoaña et al., 2003, 2008). Accordingly, a mineral dust contribution to loess sediments of the Carpathain Basin is supposed. Indeed, as it is demonstrated by the Late Pleistocene background dust concentration (Varga et al., IN PRESS) and Sr-Nd isotope database for the CB (Újvári et al., 2012), an admixture of Saharan dust into loess cannot be dismissed, however significant contribution of North African material seems to be unlikely based on grain size considerations.

The relationship between large-scale quasi-periodic climate patterns (El Niño Southern Oscillation, North Atlantic Oscillation) and Saharan dust emission is controversial. As proposed by Prospero and Lamb (2003), large dust outbreaks could be associated with major El Niño events. During the Pliocene, a permanent El Niño-like state (El Padre) has influenced the climate conditions (Ravelo et al., 2006; Shukla el al., 2009), thus the Saharan dust outbreaks could be more dominant factors in Pliocene dust accumulations in the CB which material subsequently preserved as red clay in the basin.

4. Conclusions

A multi-year record of various data sources including TOMS Aerosol Index, satellite images, HYSPLIT backward trajectory counting and synoptical meteorology were used to identify and analyse Saharan dust events in the CB atmosphere over the period of 1979–2011. In this period, 130 SDEs were detected altogether, primarily during spring and summer. Based on the daily geopotential height, wind flow and meridional wind vector maps of dusty days, the SDEs were classified into three main types. In the case of Type-1, a trough emanates from the direction of Bay of Biscay to the Atlantic coast of Africa. The eastern cell of the divided subtropical high and the cyclonic stream of a low-pressure system cause the strong SW flow. During Type-2 events, dust transportation can be connected to the warm sector winds on the foreside of an eastern moving Mediterranean cyclone. The relatively seldom Type-3 events are responsible for the longest dust transportation from the western parts of the Sahara along the western fringe of an anticyclone and by the westerlies.
Our results nicely demonstrate that Saharan dust could often be detected in the CB atmosphere. SDEs, during the dustier periods of the Pliocene and Pleistocene could have served as significant source of clay and fine silt particles which then may have contributed to the widely distributed aeolian dust deposits in the basin.

Acknowledgement

This contribution was made possible through financial support by “Developing Competitiveness of Universities in the South Transdanubian Region (SROP-4.2.1.B-10/2/KONV-2010-0002)”. The authors gratefully acknowledge the NOAA Air Resources Laboratory (ARL) for the provision of the HYSPLIT transport model and READY website (http://www.arl.noaa.gov/ready.php) used in this publication. The composite

maps of geopotential height and wind vectors were provided by the NOAA/ESRL Physical Sciences Division, Boulder Colorado from their Web site at http://www.esrl.noaa.gov/psd/.

References

Arimoto, R., 2001. Eolian dust and climate: relationships to sources, tropospheric chemistry, transport and deposition. Earth-Science Reviews 54, 29–42.

Atalay, I., 1997. Red Mediterranean soils in some karstic regions of Taurus mountains, Turkey. Catena 28, 247−260.

Barkan, J., Alpert, P., Kutiel, H., Kishcha, P., 2005. Synoptics of dust transportation days from Africa toward Italy and central Europe. Journal of Geophysical Research. Atmospheres 110, D07208. 14 p.

Barkan, J., Alpert, P., 2010. Synoptic analysis of a rare event of Saharan dust reaching the Arctic region. Weather 65, 208–211.

Borbély-Kiss, I., Kiss, Á.Z., Koltay, E., Szabó, G., Bozó, L., 2004. Saharan dust episodes in Hungarian aerosol: elemental signatures and transport trajectories. Journal of Aerosol Science 35., 1205–1224.

Cremaschi, M., 1990a. Stratigraphy and palaeoenvironmental significance of the loess deposits on Susak Island (Dalmatian archipelago). Quaternary International 5, 97–106.

Cremaschi, M., 1990b. The loess in northern and central Italy; a loess basin between the Alps and the Mediterranean regions. In: Cremaschi, M. (ed): The loess in northern and central Italy; a loess basin between the Alps and the Mediterranean region (guidebook to the excursion in northern and central Italy, September-October 1988). Pubblicazione, Dipartimento de Scienze della Terra dell'Universita degli Studi Milano. Sezione di Geologia e Paleontologia, Nuova Serie 602, 15–19.

D'Almeida, G.A., 1986. A model of Saharan dust transport. Journal of Applied Meteorology 25, 903–916.

Dayan, U., Shoob, T., Enzel, Y., Ziv, B., 2007. Suspended dust over southeastern Mediterranean and its relation to atmospheric circulations. International Journal of Climatology 28, 915–924.

Draxler, R.R., Hess, G.D., 1997. Description of the HYSPLIT_4 modeling system. NOAA Tech. Memo. ERL ARL-224, NOAA Air Resources Laboratory, Silver Spring, MD, 24 p.

Draxler, R.R., Rolph, G.D., 2012. HYSPLIT (HYbrid Single-Particle Lagrangian Integrated Trajectory) Model access via NOAA ARL READY Website (http://ready.arl.noaa.gov/HYSPLIT.php). NOAA Air Resources Laboratory, Silver Spring, MD.

Durn, G., Ottner, F., Slovenec, D., 1999. Mineralogical and geochemical indicators of the polygenetic nature of terra rossa in Istria, Croatia. Geoderma 91, 125–150.

Engelstaedter, S., Tegen, I., Washington, R., 2006. North African dust emissions and transport. – Earth-Science Reviews 79, 73–100.

Franzén, L.G., Hjelmroos, M., Kallberg, P., Brorstrom-Lunden, E., Junitto, S., Savolainen, A., 1994. The yellow snow episode of Northern Fennoscandia, March 1991 – a case study of long-distance transport of soil, pollen and stable organic compounds. Atmospheric Environment 28, 3587–3604.

Gerasopoulos, E., Kouvarakis, G., Babasakalis, P., Vrekoussis, M., Putaud, J.P., Mihalopoulos, N., 2006. Origin and variability of particulate matter (PM_{10}) mass concentrations over the Eastern Mediterranean. Atmospheric Environment 40, 4679–4690.

Ginoux, P.M., Chin, I., Tegen, I., Prospero, J., Holben, M., Dubovik, O., Lin, S.J., 2001. Global simulation of dust in the troposhere: model description and assessment. Journal of Geophysical Research 106, 20255−20273.

Gillette, D.A., 1999. A qualitative geophysical explanation for "hot spot" dust emitting source regions. Contributions to Atmospheric Physics 72, 67–77.

Glaccum, R.A., Prospero, J.M., 1980. Saharan aerosols over the tropical North Atlantic: mineralogy. Marine Geology 37, 295–321.

Goudie, A.S., Middleton, N.J., 2006. Desert Dust in the Global System. Springer, 287 p.

Griffin, D.W., Kellogg, C.A., Shinn, E.A., 2001. Dust in the wind: Long range transport of dust in the atmospere and its implications for global public and ecosystem health. Global Change and Human Health 2, 20–33.

Hamonou, E., Chazette, P., Balis, D., Dulac, F., Schneider, X., Galani, E., Ancellet, G., Papayannis, A., 1999. Characterization of the vertical structure of Saharan dust export to the Mediterranean basin. Journal of Geophysical Research. Atmospheres 104, 22257–22270.

Harrison, S.P., Kohfeld, K.E., Roelandt, C., Claquin, T., 2001. The role of dust in climate changes today, at the last glacial maximum and in the future. Earth-Science Reviews 54, 43–80.

Herman, J.R., Bhartia, P.K., Torres, O., Hsu, C., Seftor, C., Celarier, E., 1997. Global distribution of UV-absorbing aerosols from Nimbus 7 TOMS data. Journal of Geophysical Research Atmospheres 102, 16911–16922.

Hoogakker, B.A.A., Rothwell, R.G., Rohling, E.J., Paterne, M., Stow, D.A.V., Herrle, J.O., Clayton, T., 2004. Variations in terrigenous dilution in western Mediterranean Sea pelagic sediments in response to climate change during the last glacial cycle. Marine Geology 211, 21–43.

Israelevich, P.L., Levin, Z., Jospeh, J.H., Ganor, E., 2002. Desert aerosol transport in the Mediterranean region inferred from the TOMS aeosol index. Journal of Geophysical Research. Atmospheres 107(D21), 4572, 13 p.

Jackson, M.L., Clayton, R.N., Violante, A., Violante, P., 1982. Eolian influence on terra rossa soils of Italy traced by quartz oxygen isotopic ratio. In: van Olphen, H., Veniale, F., (eds.): International Clay Conference, Bologna and Pavia, Italy, September 1981, Elsevier, Amsterdam, 293-300.

Jahn, R., Zarei, M., Stahr, K., 1991. Genetic implications of quartz in “Terra Rossa”-soils in Portugal. Proceedings of 7th Euroclay Conference, Dresden, 541–546.

Kalnay, E., Kanamitsu, M., Kistler, R., Collins, W., Deaven, D., Gandin, L., Iredell, M., Saha, S., White, G., Woollen, J., Zhu, Y., Leetmaa, A., Reynolds, B., Chelliah, M., Ebisuzaki, W., Higgins, W., Janowiak, J., Mo, K. C., Ropelewski, C., Wang, J., Jenne, R., Joseph, D., 1996. The NCEP/NCAR 40-Year Reanalysis Project. Bulletin of the American Meteorological Society 77, 437–471.

Kiss, P., Jánosi, I., Torres, O., 2007. Early calibration problems detected in TOMS Earth-Probe aerosol signal. Geophysical Research Letters 34. (7) L07803. 5 p.

Klein, H., Nickovic, S., Haunold, W., Bundke, U., Nillius, B., Ebert, M., Weinbruch, S., Schuetz, L., Levin, Z., Barrie, L.A., Bingemer, H., 2010. Saharan dust and ice nuclei over Central Europe. Atmospheric Chemistry and Physics 10, 10211–10221.

Kohfeld, K.E., Harrison, S.P., 2001. DIRTMAP: the geological record of dust. Earth-Science Reviews 54, 81–114.

Kohfeld, K.E., Tegen, I., 2007. Record of Mineral Aerosols and Their Role in the Earth System. Treatise on Geochemistry 4, pp. 1–26

Koltay, E., Borbély-Kiss, I., Kertész, Zs., Kiss, Á.Z., Szabó, Gy., 2006. Assignment of Saharan dust sources to episodes in Hungarian atmosphere by PIXE and TOMS observations. Journal of Radioanalytical and Nuclear Chemistry 267, 449–459.

Kovács, J., 2008. Grain-size analysis of the Neogene red clay formation in the Pannonian Basin. International Journal of Earth Sciences 97, 171–178.

Kovács, J., Varga, Gy., Dezső, J., 2008. Comparative study on the Late Cenozoic red clay deposits from China and Central Europe (Hungary). Geological Quarterly 52, 369–382.

Kovács, J., Fábián, Sz.Á., Varga, G., Újvári, G., Varga, Gy., Dezső, J., 2011. Plio−Pleistocene red clay deposits in the Pannonian Basin: A review. Quaternary International 240, 35–43.

Larrasoaña, J.C., Roberts, A.P., Rohling, E.J., Winklhofer, M., Wehausen, R., 2003. Three million years of monsoon variability over the northern Sahara. Climate Dynamics 21, 689–698.

Larrasoaña, J.C., Roberts, A.P., Rohling, E.J., 2008. Magnetic susceptibility of eastern Mediterranean marine sediments as a proxy for Saharan dust supply? Marine Geology 254, 224–229.

MacLeod, D.A., 1980. The origin of the red Mediterranean soils in Epirus, Greece. Journal of Soil Science 31, 125–136.

Maher, B.A., Prospero, J.M., Mackie, D., Gaiero, D., Hesse, P.P., Balkanski, Y., 2010. Global connenctions between aeolian dust, climate and ocean biogeochemistry at the present day and at the last glacial maximum. Earth-Science Reviews 99, 61–97.

Mahowald, N., Kohfeld, K., Hansson, M., Balkanski, Y., Harrison, S.P., Prentice, I.C., Schulz, M., Rodhe, H., 1999: Dust sources and deposition during the last glacial maximum and current climate: a comparison of model results with paleodata from ice cores and marine sediments. Journal of Geophysical Research 104, 15895−15916.

Mahowald, N.M., Muhs, D.R., Levis, S., Rasch, P.J., Yoshioka, M., Zender, C.S., Luo, C., 2006. Change in atmospheric mineral aerosols in response to climate: Last glacial period, preindustrial, modern, and doubled carbon dioxide climates. Journal of Geophysical Research 111. D10202. 22 p.

Matassoni, L., Pratesi, G., Centioli, D., Cadoni, F., Lucarelli, F., Nava, S., Malesani, P., 2011. Saharan dust contribution to PM_{10}, $PM_{2.5}$ and PM_1 in urban and suburban areas of Rome: A comparison between single-particle SEM-EDS analysis and whole-sample PIXE analysis. Journal of Environmental Monitoring 13, 732–742.

McTainsh, G.H., Walker, P.H., 1982. Nature and distribution of Harmattan dust. Zeitschrift für Geomorphologie 26, 417–435.

Middleton, N.J., Goudie, A.S., 2001. Saharan dust: sources and trajectories. Transactions of the Institute of British Geographers NS 26, 165–181.

Mill, H.R.J., Lempfert, R.G.K., 1904. The great dust-fall of February 1903, and its origin. Quarterly Journal of the Royal Meteorological Society 30, 57–73.

Miller, R.L., Tegen I., Perlwitz, J., 2004. Surface radiative forcing by soil dust aerosols and the hydrologic cycle. Journal of Geophysical Research. Atmospheres 109, D04203, 24 p.

Moreno, A., Cacho, I., Canals, M., Prins, M.A., Sánchez-Goñi, M.F., Grimalt, J.O., Weltje, G.J., 2002. Saharan dust transport and high-latitude glacial climatic variability: The Alboran Sea record. Quaternary Research 58, 318–328.

Moulin, C., Lambert, C.E., Dayan, U., Masson, V., Ramonet, M., Bousquet, P., Legrand, M., Balkanski, Y.J., Guelle, W., Marticorena, B., Bergametti, G., Dulac, F., 1998. Satellite climatology of African dust transport in the Mediterranean atmosphere. Journal of Geophysical Research. Atmospheres 103. (D11), 13137–13143.

Muhs, D.R., Bettis, E.A., 2003. Quaternary loess–paleosol sequences as examples of climate-driven sedimentary extremes. Geological Society of America Special Paper 370, 53–74.

Muhs, D.R., Budahn, J., Avila, A., Skipp, G., Freeman, J., Patterson, DeA., 2010. The role of African dust in the formation of Quaternary soils on Mallorca, Spain and implications for the genesis of Red Mediterranean soils. Quaternary Science Reviews 29, 2518–2543.

Pécsi, M. 1990. Loess is not just the accumulation of dust. Quaternary International 7–8, 1–21.

Pécsi, M., Schweitzer, F. 1993. Long-term terrestrial records of the middle Danubian Basin. Quaternary International 17, 5–14.

Pósfai, M., Buseck, P.R., 2010. Nature and climate effects of individual tropospheric aerosol particles. Annual Review of Earth and Planetary Sciences 38, 17–43.

Prospero, J.M., 1996. Saharan dust transport over the north Atlantic Ocean and Mediterranean: An overview. In: Guerzoni, S., Chester, R. (eds.): The impact of desert dust across the Mediterranean, October 1995, Oristano, Italy, Environmental Science and Technology Library 11, Dordrecht and London: Kluwer, 133–152.

Prospero, J.M., Ginoux, P.M., Torres, O., Nicholson, S.E., Gill, T.E. 2002. Environmental characterization of global sources of atmospheric soil dust identified with the Nimbus-7 Total Ozone Mapping Spectrometer (TOMS) absorbing aerosol product. Reviews of Geophysics 40, 31 p.

Prospero, J.M., Lamb, P.J., 2003. African droughts and dust transport to the Caribbean: Climate change implications. Science 302, 1024–1027.

Psenner, R., 1999. Living in a dusty world: airborne dust as a key factor for alpine lakes. Water, Air, and Soil Pollution 112, 217–227.

Pye, K., 1987. Aeolian Dust and Dust Deposits. Academic Press, London, 334 p.

Pye, K., 1995. The nature, origin and accumulation of loess. Quaternary Science Reviews 14, 653–667.

Ravelo, C.A., Dekens, S.P., McCarthy, M., 2006: Evidence for El Niño-like conditions during the Pliocene. GSA Today 16, 4–11.

Ridgwell, A.J., 2002. Dust in the Earth system: The biogeochemical linking of land, air, and sea. Philosophical Transactions. Series A, Mathematical, physical, and engineering sciences 360, 2905–2924.

Roda, F., Bellot, J., Avila, A., Escarre, A., Pinol, J., Terradas, J., 1993. Saharan dust and the atmospheric inputs of elements and alkalinity to Mediterranean ecosystems. Water, Air, and Soil Pollution 66, 277–288.

Rodríguez, S., Querol, X., Alastuey, A., Kallos, G., Kakaliagou, O., 2001. Saharan dust contributions to PM_{10} and TSP levels in Southern and Eastern Spain. Atmospheric Environment 35, 2433–2447.

Rogora, M., Mosello, R., Marchetto, A., 2004. Long-term trends in the chemistry of atmospheric deposition in northwestern Italy: the role of increasing Saharan dust deposition. Tellus B 56, 426–434.

Rolph, G.D., 2012. Real-time Environmental Applications and Display sYstem (READY) Website (http://ready.arl.noaa.gov). NOAA Air Resources Laboratory, Silver Spring, MD.

Rosenfeld, D., Rudich, Y., Lahav, R., 2001. Desert dust suppressing precipitation: A possible desertification feedback loop. The Proceedings of the National Academy of Sciences of the United States of America 98, 5975–5980.

Rousseau, D.D., Derbyshire, E., Antoine, P., Hatté, C., 2007. Loess records, Europe. In: Elias, S.A. (ed), Encyclopedia of Quaternary science, vol. 2, Amsterdam: Elsevier, 1440–1456.

Rózycki, S.Z., 1991. Loess and loess-like deposits: evolution of views on the genesis of loess; classical loess provinces; loess of the warm zone. Ossolineum, Wroclaw, 170 p.

Sassen, K., DeMott, P.J., Prospero, J.M., Poellot, M.R., 2003. Saharan dust storms and indirect aerosol effects on clouds: CRYSTALFACE results. Geophysical Research Letters 30. (12), 1633, 4 p.

Shukla, S.P., Chandler, M.A., Jonas, J., Sohl, L.E., Mankoff, K., Dowsett, H., 2009: Impact of permanent El Niño (El Padre) and Indian Ocean Dipole in warm Pliocene climates. Paleoceanography 24. PA2221. 12 p.

Špoler Čanić, K., Vidič, S., Klaić, Z.B., 2009. Precipitation chemistry in Croatia during the period 1981–2006. Journal of Environmental Monitoring 11, 839–851.

Stout, J.E., Warren, A., Gill, T.E., 2009. Publication trends in aeolian research: an analysis of the Bibliography of Aeolian Research. Geomorphology 105, 6–17

Stuut, J-B.W., Smalley, I., O'Hara-Dhand, K., 2009. Aeolian dust in Europe: African sources and European deposits. Quaternary International 198, 234–245.

Sun, D., Bloemendal, J., Rea, D.K., Vandenberghe, J., Jiang, F., An, Z., Su, R., 2002. Grain-size distribution function of polymodal sediments in hydraulic and aeolian environments, and numerical partitioning of the sedimentary components. Sedimentary Geology 152, 263–277.

Sun, D., Bloemendal, J., Rea, D.K., An, Z., Vandenberghe, J., Lu, H., Su, R., Liu, T.S., 2004. Bimodal grain-size distribution of Chinese loess, and its paleoclimatic implications. Catena 55, 325–340.

Szoboszlai, Z., Kertész, Z., Szikszai, Z., Borbély-Kiss, I., Koltay, E., 2009. Ion beam microanalysis of individual aerosol particles originating from Saharan dust episodes observed in Debrecen, Hungary. Nuclear Instruments and Methods in Physics Research Section B: Beam Interactions with Materials and Atoms 267, 2241–2244.

Tegen, I., Lacis, A.A., Fung, I., 1996. The influence of mineral aerosols from disturbed soils on climate forcing. Nature 380, 419–422.

Torres, O., Bhartia, P.K., Herman, J.R., Ahmad, Z., Gleason, J., 1998. Derivation of aerosol properties from a satellite measurements of backscattered ultraviolet radiation: Theoretical basis. Journal of Geophysical Research Atmospheres 103. (D14) 17099–17110.

Tsoar, H., Pye, K., 1987. Dust transport and the question of desert loess formation. Sedimentology 34, 134–153.

Tullet, M.T., 1978. A dust fall on 6 March 1977. Weather 33, 48–52.

Újvári, G., Kovács, J., Varga, Gy., Raucsik, B., Markovic, S.B., 2010. Dust flux estimates for the Last Glacial Period in East Central Europe based on terrestrial records of loess deposits: A review. Quaternary Science Reviews 29, 3157–3166.

Újvári, G., Varga, A., Ramos, F.C., Kovács, J., Németh, T., Stevens, T., 2012. Evaluating the use of clay mineralogy, Sr-Nd isotopes and zircon U-Pb ages in tracking dust provenance: an example from loess of the Carpathian Basin. Chemical Geology 304–305, 83–96.

Varga, Gy., 2011. Similarities among the Plio–Pleistocene terrestrial aeolian dust deposits in the world and in Hungary. Quaternary International 234, 98–108.

Varga, Gy., Kovács, J., Újvári, G., (in press). Late Pleistocene variations of the background aeolian dust concentration in the Carpathian Basin: an estimate using decomposition of grain-size distribution curves of loess deposits. Netherlands Journal of Geosciences,

Vernon, P.D., Reville, W.J., 1983. The dustfall of November 1979. Journal of Earth sciences Royal Dublin Society 5, 135–144.

Washington, R.,Todd, M., Middleton, N.J., Goudie, A.S., 2003. Dust-storm source areas determined by the Total Ozone Monitoring Spectrometer and surface observations. Annals of the Association of American Geographers 93, 297–313.

Yaloon, D.H., 1997: Soils in the Mediterranean region: what makes them different? Catena. 28, 157–169.

Wheeler, D.A., 1986. The meteorological background to the fall of Saharan dust, November 1984. Meteorological Magazine 115, 1–9.

Figures

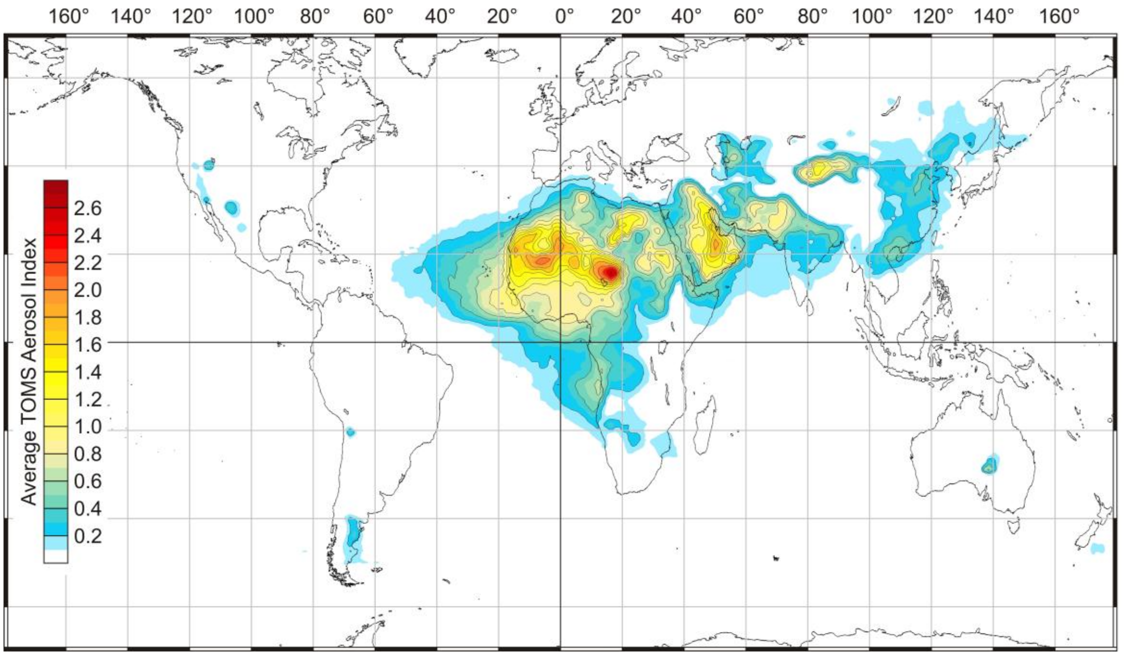

Figure 1. Mean global TOMS AI map of the investigated 23 full years from 1979 to 2009.

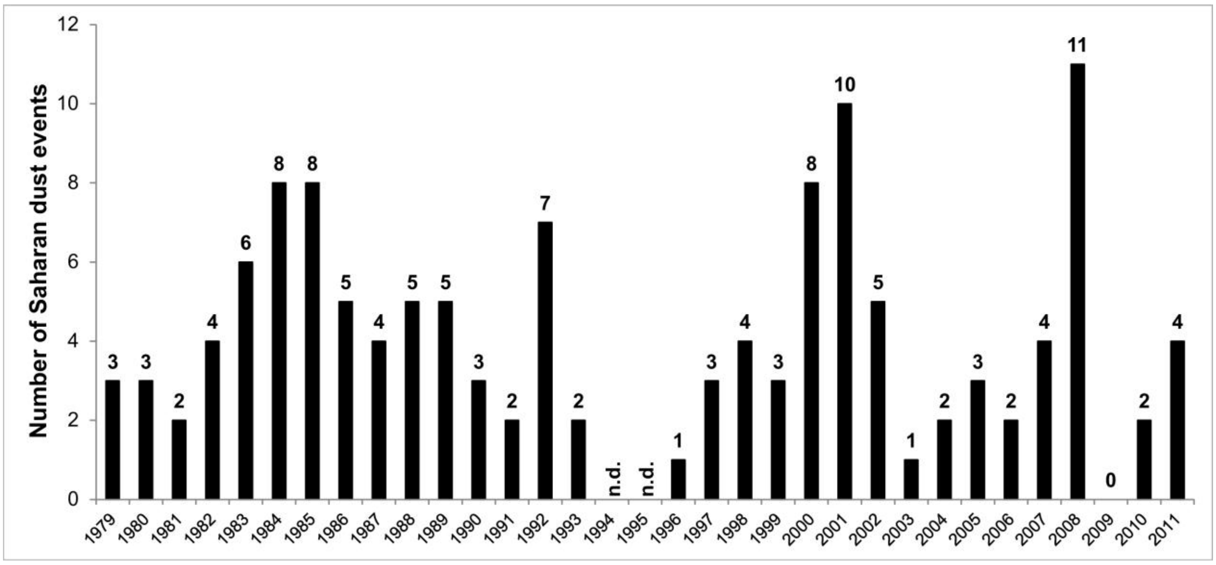

Figure 2. Annual number of identified Saharan dust intrusions in the atmosphere of the Carpathian Basin. The data from years of 1993 and 1996 are fractional; n.d. means no data.

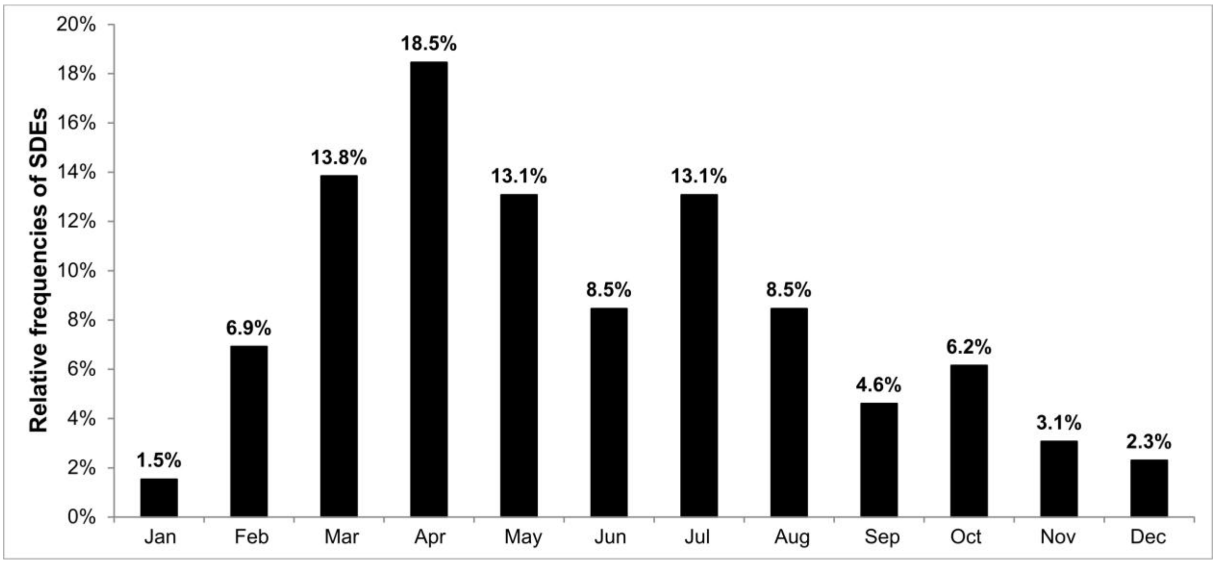

Figure 3. The seasonality of identified North African dust episodes over the Carpathian Basin (1979–2009).

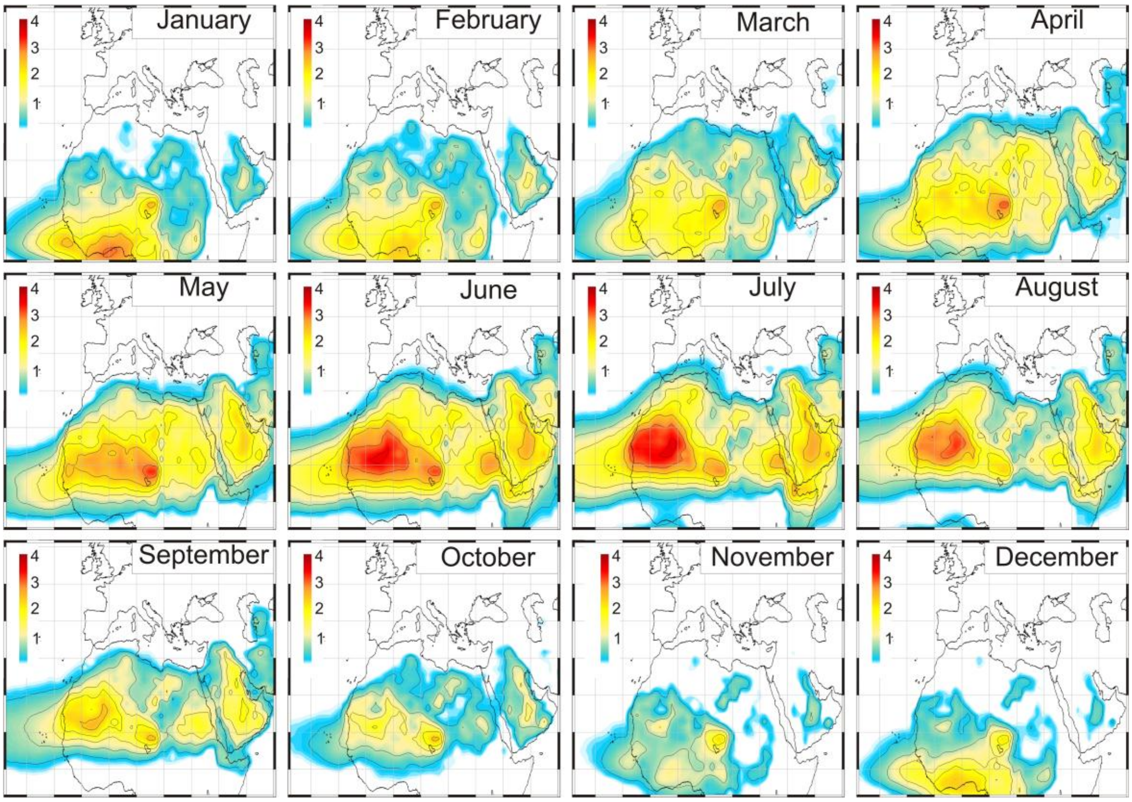

Figure. 4. Monthly mean TOMS AI maps of North Africa (1979–2009).

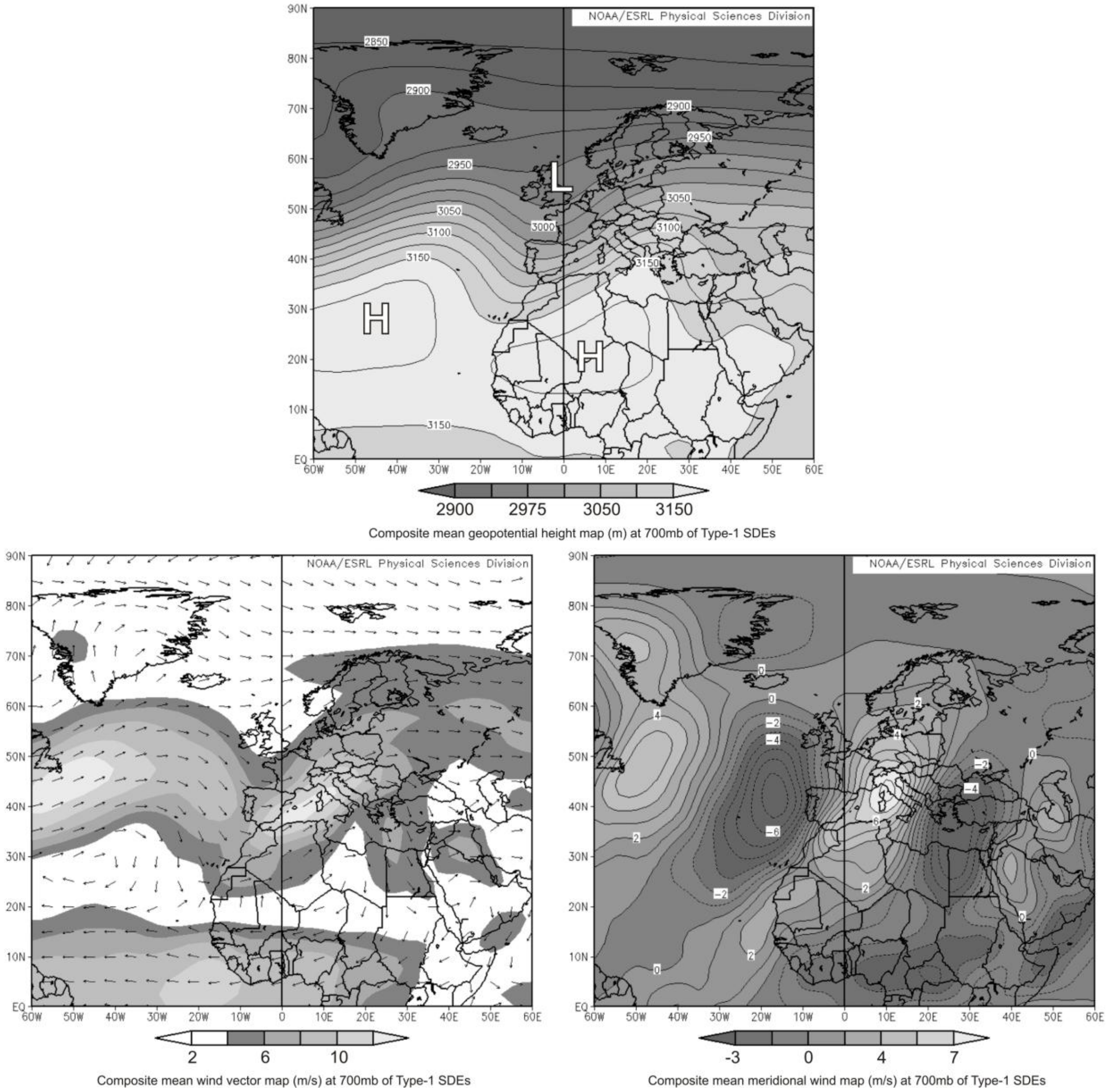

Figure 5. Composite mean maps of the Type-1 synoptic situations (n=86).

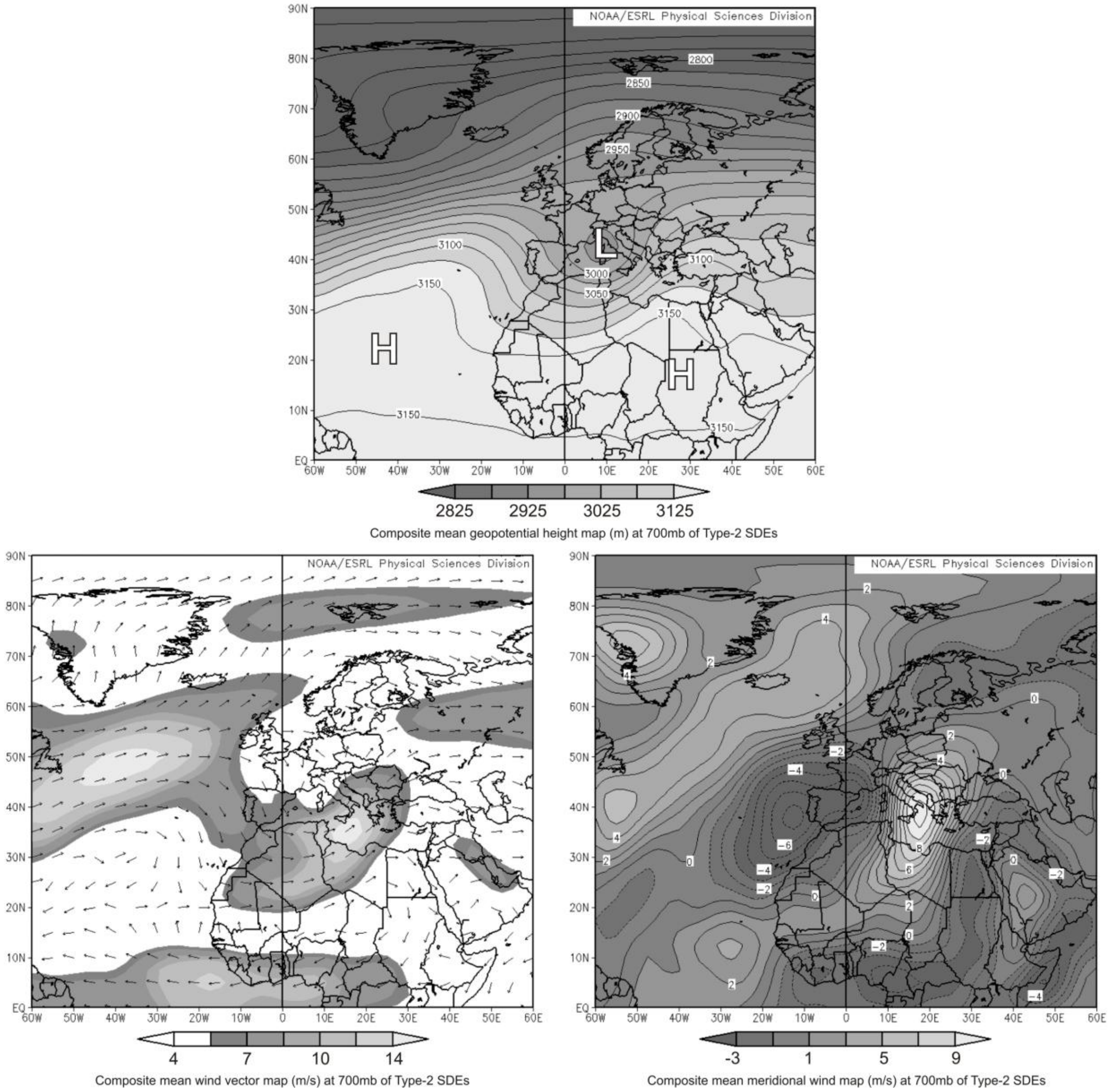

Figure 6. Composite mean maps of the Type-2 synoptic situations (n=33).

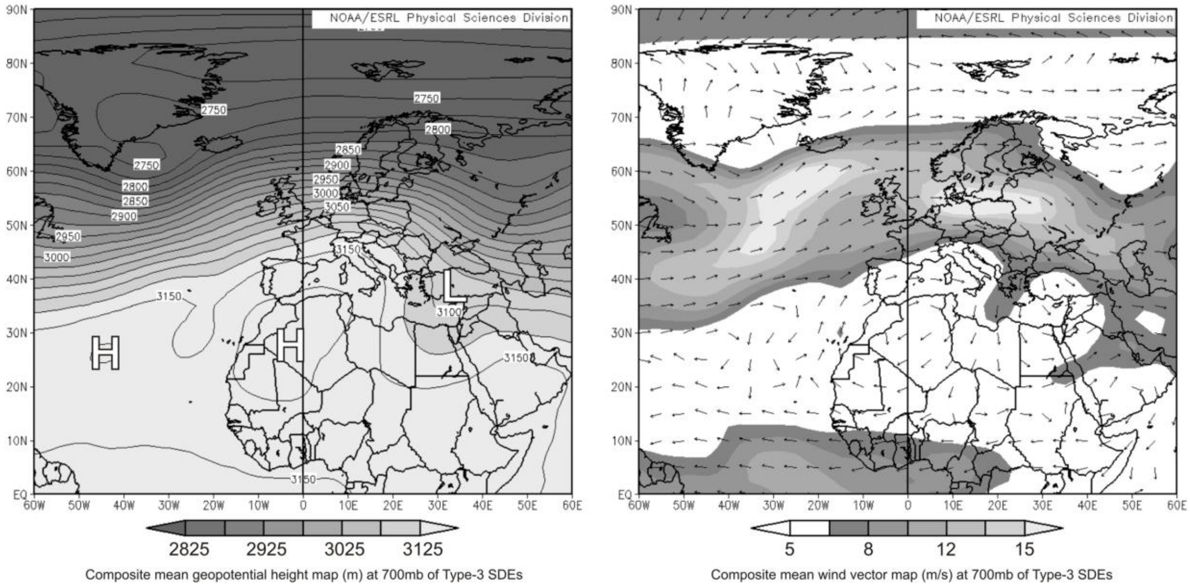

Figure 7. Composite mean maps of the Type-3 synoptic situations (n=11).

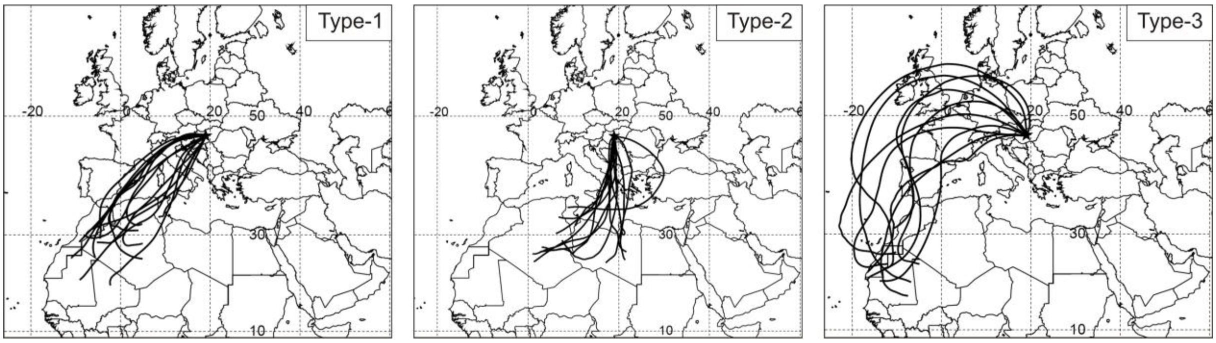

Figure 8. Typical pathways of dust transport trajectories toward the Carpathian Basin.

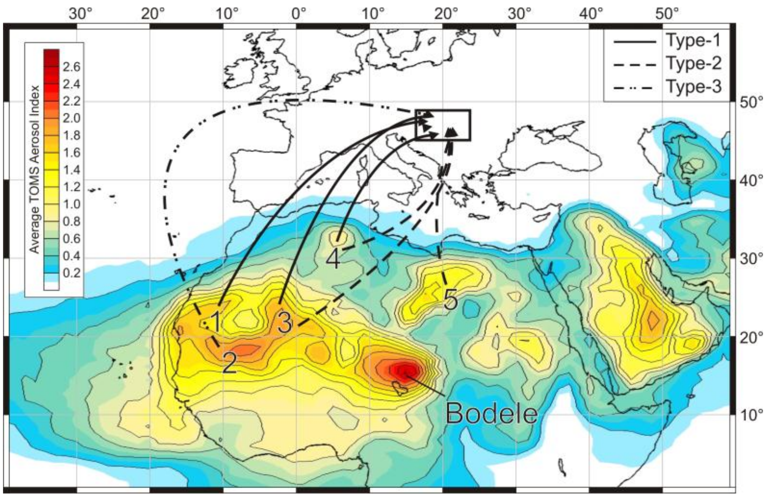

Figure 9. Major source areas and schematic transport routes of Saharan dust identified over the Carpathian Basin (the numbers are explained in the text).